Quantification of Lithium via Redox Titration and pH Titration – A Method Comparison

by
Joseph J. Hebert

A THESIS

submitted to

Oregon State University

Honors College

in partial fulfillment of
the requirements for the
degree of

Honors Baccalaureate of Science in Chemical Engineering and Chemistry
(Honors Associate)

Presented May 26, 2020
Commencement June 2020

AN ABSTRACT OF THE THESIS OF

Joseph J. Hebert for the degree of Honors Baccalaureate of Science in Chemical Engineering and Chemistry presented on May 26, 2020. Title: Quantification of Lithium via Redox Titration and pH Titration - A Method Comparison.

Abstract approved:_____

Michael Lerner

Lithium serves an unparalleled role for high energy-density storage applications and is vital for the continued advancement of the world economy. However, global supply is heavily reliant on lithium deposits situated in select locations, creating unpredictability in the price and concerns for the sustained production of the resource. Additionally, future demands for applications in the small electronics, automotive, and renewable energy industries threaten to place further strain on the lithium supply. Thus, the implementation of lithium battery recycling methods is critical meet this expected surge in demand for lithium-based battery technologies. Several economic obstacles and safety considerations have halted the advancement of these necessary recycling techniques. A prominent barrier to recycling efforts revolves around the reactivity of active lithium compounds that remain in used lithium batteries. As a result, significant safety precautions must be taken when handling and transporting lithium-based batteries, adding to the costs associated with recycling methods. Current research has been dedicated to developing a passivation method for the remaining active lithium in used cells, seeking to lower the classification, and subsequently the costs, associated with these materials. Analytical techniques, which quantify the amount of active lithium separate from compounds associated with passivation, require development to prove the functionality of passivation methods. This study focuses on two potential chemistries, a redox titration with triiodide and a pH titration with a strong acid, which serve as cost-effective and robust methods for quantifying active lithium. Lithium was determined to be a suitable reductant for triiodide to iodide by UV/vis analysis, with the characteristic triiodide

peaks disappearing over time when in the presence of lithium metal. However, significant drawbacks resulting from the large difference in molar masses between lithium and triiodide and the competing reductant properties of copper, a common material used for anode current collectors, render the method impractical for quantifying the amount of active lithium in lithium batteries. Preliminary studies for the pH titration exhibited positive results, with repeated success in using sulfuric acid to accurately measure the amount of lithium hydroxide and lithium methoxide present in solution, which would result from the reaction of lithium metal with water and methanol, respectively. Unforeseen circumstances, however, halted the continuation of the pH titration method development and further studies around potential contaminants and undesired reactions must be conducted to determine the feasibility of the technique.

Key Words: Lithium Content, Lithium Battery Recycling, Lithium Quantification, pH Titration, Redox Titration

Corresponding e-mail address: hebertjo@oregonstate.edu

Quantification of Lithium via Redox Titration and pH Titration - A Method Comparison

by
Joseph J. Hebert

A THESIS

submitted to

Oregon State University

Honors College

in partial fulfillment of
the requirements for the
degree of

Honors Baccalaureate of Science in Chemical Engineering and Chemistry
(Honors Associate)

Presented May 26, 2020
Commencement June 2020

Honors Baccalaureate of Science in Chemical Engineering and Chemistry project of Joseph J. Hebert presented on May 26, 2020.

APPROVED:

_____

Michael Lerner, Mentor, representing Department of Chemistry

_____

Zhenxing Feng, Committee Member, representing Department of Chemical Engineering

_____

Steve Sloop, Committee Member, representing OnTo Technology LLC

_____

Toni Doolen, Dean, Oregon State University Honors College

I understand that my project will become part of the permanent collection of Oregon State University, Honors College. My signature below authorizes release of my project to any reader upon request.

_____

Joseph J. Hebert, Author

Quantification of Lithium via Redox Titration and pH Titration – A Method Comparison

Joseph J. Hébert[1*], Lauren Crandon[2], Steve Sloop[2], Michael M. Lerner[1]

hebertjo@oregonstate.edu

[1]*Department of Chemistry, Oregon State University, Gilbert Hall, Corvallis, Oregon 97331*
[2]*Onto Technology LLC, 63221 Service Road Suite F, Bend, Oregon 97703*

Abstract.

Lithium serves an unparalleled role for high energy-density storage applications and is vital for the continued advancement of the world economy. However, global supply is heavily reliant on lithium deposits situated in select locations, creating unpredictability in the price and concerns for the sustained production of the resource. Additionally, future demands for applications in the small electronics, automotive, and renewable energy industries threaten to place further strain on the lithium supply. Thus, the implementation of lithium battery recycling methods is critical meet this expected surge in demand for lithium-based battery technologies. Several economic obstacles and safety considerations have halted the advancement of these necessary recycling techniques. A prominent barrier to recycling efforts revolves around the reactivity of active lithium compounds that remain in used lithium batteries. As a result, significant safety precautions must be taken when handling and transporting lithium-based batteries, adding to the costs associated with recycling methods. Current research has been dedicated to developing a passivation method for the remaining active lithium in used cells, seeking to lower the classification, and subsequently the costs, associated with these materials. Analytical techniques, which quantify the amount of active lithium separate from compounds associated with passivation, require development to prove the functionality of passivation methods. This study focuses on two potential chemistries, a redox titration with triiodide and a pH titration with a strong acid, which serve as cost-effective and robust methods for quantifying active lithium. Lithium was determined to be a suitable reductant for triiodide to iodide by UV/vis analysis, with the characteristic triiodide peaks disappearing over time when in the presence of lithium metal. However, significant drawbacks resulting from the large difference in molar masses between lithium and triiodide and the competing reductant properties of copper, a common material used for anode current collectors, deemed the method impractical for quantifying the amount of active lithium in lithium batteries. Preliminary studies for the pH titration exhibited positive results, with repeated success in using sulfuric acid to accurately measure the amount of lithium hydroxide and lithium methoxide present in solution, which would result from the reaction of lithium metal with water and methanol, respectively. Unforeseen circumstances, however, halted the continuation of the pH titration method development and further studies around potential contaminants and undesired reactions must be conducted to determine the feasibility of the technique.

Background.

In the latter half of the 20th century, lithium has become of significant interest for use in high energy-density applications, most prominently in lithium-based batteries.[1] It should be noted that the use of the phrase lithium and lithium-based battery encompasses both lithium-primary and lithium-ion battery technologies. While lithium is the lightest metal and least dense solid element in the periodic table, perhaps its most significant characteristic is its high electrochemical potential.[1] These properties are ideal for a range of technological applications, such as cell phones, computers, and automobiles, where the energy demand is large and weight must be conserved. Other chemical storage options, such as alkaline or lead-acid battery technologies, fall short of meeting the power requirement, or require significant amounts of materials to meet the application needs, when compared to lithium-based battery technologies. As shown in **Figure 1** below, lithium-based batteries possess the highest power and energy potential per mass when compared to other, conventional technologies.[2] With such unique characteristics and significant charge to mass ratio, a replacement for lithium in high performance battery technologies is unlikely. However, as economies continue to advance, the demand for batteries is expected to increase, bringing with it concern for possible shortages in the global supply of lithium and associated materials.

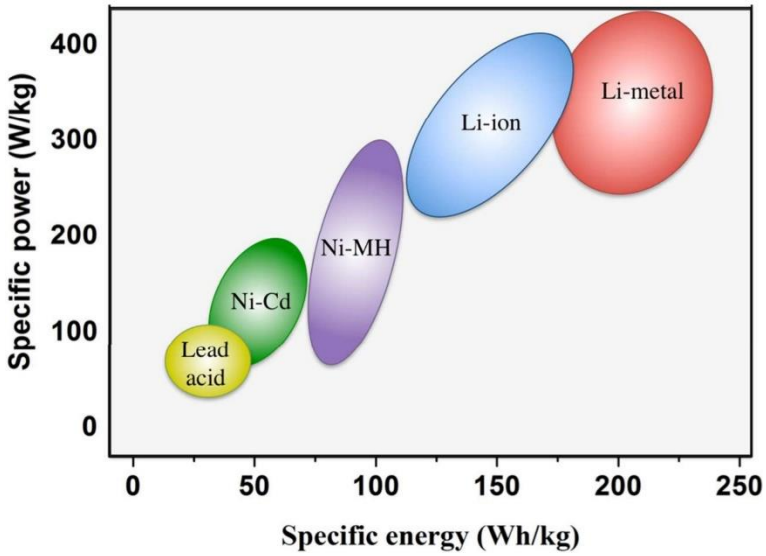

Figure 1. Ragone plot for a range of battery technologies comparing the specific power (W/kg) to the specific energy (Wh/kg) potential. Li-metal used in the figure above refers to lithium-primary battery technology. [figure from Meesala, Y.; Jena, A.; Chang, H.; Liu, R.-S., Recent Advancements in Li-Ion Conductors for All-Solid-State Li-Ion Batteries. *ACS Energy Letters* **2017,** *2* (12), 2734-2751.]

It is estimated that 39 million metric tons of lithium make up the global deposits, which is nearly 300,000 times the present annual production.[3] Currently, lithium is obtained through two critical pathways, either mining of an aluminosilicate mineral of lithium called spodumene or pumping of lithium chloride found in brine lake deposits.[1, 3] The liberation of lithium from spodumene and other minerals requires energy intense processes that utilize extreme temperatures and harsh chemicals.[4] Thus, extraction of lithium through brine lake deposits is significantly more cost effective, producing far fewer emissions. However, only 58% of the

global supply of lithium is contained in brine lake deposits.[3] In addition, all sources of lithium are found in only a few select locations, with approximately 75% the world's known lithium supply contained in the salt lakes of Argentina, Bolivia, and Chile, as shown below in **Figure 2**.[3] As a result, the world economy is heavily dependent on these countries for the continued supply of lithium. While arguments have been made over the development position of these countries, their economies remain unpredictable, generating concerns over the stability of the global price for lithium. The United States, for example, is heavily reliant on other countries for their lithium supply, with over 70% of the consumed lithium generated from imports.[3] Thus, companies in the United States and Asia have started to form strategic alliances to ensure the security of the vital resource.[5] As a result, the United States Geological Survey (USGS) considers lithium to be a critical or near-critical element for its importance in future green technologies and advancing economies.[3]

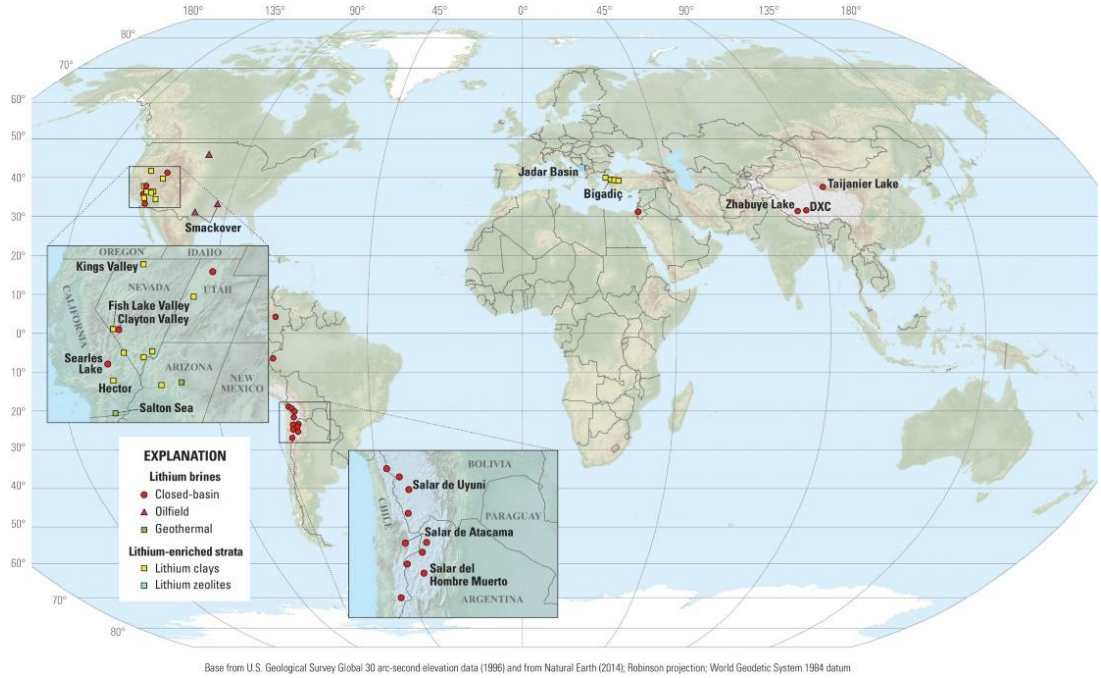

Figure 2. World map illustrating known locations of lithium deposits categorized as closed-basin lithium-brine, lithium-enriched oilfield brine, geothermal brine, lithium-clay, or lithium-zeolite deposits. [figure from Bradley, D. C.; Stillings, L. L.; Jaskula, B. W.; Munk, L.; McCauley, A. D. *Lithium*; 1802K; Reston, VA, 2017; p 34.]

Current world demands for lithium have been estimated around 25,400 metric tons annually for the years of 2007 and 2008.[1] While lithium is a critical component for energy storage, only 29% of the global production of lithium is used for battery applications.[3] The glass and ceramics industry is the largest consumer of lithium, contributing 35% of the global consumption, with the lubrication and polymer production industries contributing 8% and 5%, respectively. However, the demand for lithium batteries is expected to spike in the coming years, due to an increased global commitment to reduce carbon emissions. As shown below in **Table 1**, the world leaders in the automotive manufacturing industry have verbally pledged to transition their manufacturing away from gasoline-based cars to hybrid (electrified) and electric vehicles. Additionally, in 2015 over 200 countries signed the Paris Agreement at the United Nations Climate Conference, vowing their support in reducing their country's impact on climate change.

The implementation of renewable energy sources, such as wind and solar, will also add to the increased demand for lithium-based batteries.[1] Wind and solar energy sources are highly variable, dependent on the surrounding environment, and must be coupled with an energy storage technology to level out the energy load supplied to the grid and maximize efficiency. While these advancements would greatly reduce the global carbon footprint, the current lithium production industry may not be prepared to handle the resulting surge in demand.

Manufacturer	Commitment	Committed Year
BMW Group	Generate 15% to 25% of its total sales from electrified vehicles	2025
Daimler	Offer more than 10 electric vehicle models	2022
Fiat Chrysler	Offer at least 12 electrified or electric vehicle models	2022
Ford	Offer 40 electric or electrified vehicle models	2022
General Motors	Majority of their lineup will be electric vehicles	2030
Honda	Generate all European sales from electrified vehicles	2022
Nissan	Offer 8 electric vehicle models	2022
Toyota	Generate half of its sales from electrified vehicles	2025
Volkswagen Group	Up to 40% of their total lineup will consist of electric vehicles	2030
Volvo	Generate half of its sales from electric vehicles	2025

Table 1. List of automotive manufacturers and their verbal pledges of their commitment to producing electrified and electric vehicles. Note that the phrase 'electrified vehicles' does not signify that the vehicle is powered completely by electricity whereas 'electric vehicles' does.

With a finite and unpredictable supply, serving as a key component for numerous industries, and the looming surge in future demand, the development of recycling techniques for lithium is critical for the continued advancement of the world economy. The U.S. Department of Energy (DOE) estimates that 11 million metric tons of lithium batteries will be consumed and deemed scrap by the year 2030, with less than 5% of the current used batteries being recycled.[6] It is critical to note that these estimates are based on the current circulation of lithium-based batteries, which is primarily attributed to the small electronics industry, such as cell phones and personal computers. The future demand for lithium in the automotive and grid energy storage industries require far greater amounts of the resource. For example, the battery used to power a Chevy Volt electric car requires 288 individual cells that each contain more than twice the amount of lithium found in a typical tablet device, such as an iPad.[6] As a result of these growing concerns, several countries have dedicated resources to advancing their recycling capabilities, viewing the supply gap as an economic opportunity. The lithium battery industry has been evaluated at $70 billion by the year 2030, up from $22.8 billion in the year 2016.[6, 7] The United States invested $15 million in 2019 to establish a Lithium Battery R&D Recycling Center, along with initiating a $5.5 million 'Battery Recycling Prize' to any organization that demonstrates profitability while recycling at least 90% of all lithium-based battery technologies.

Several challenges and safety hazards must be considered when handling, and subsequently recycling, lithium battery technologies. One significant obstacle, which hinders the ability for the development of a universal recycling method, is the constant evolution in the chemistry used for lithium batteries. This is most evident in the range of materials that have been implemented for lithium-ion battery technologies since 1995. In **Figure 3** below, comparison charts are provided showing the range of materials used for the cathode, anode, and electrolyte in 1995 versus 2010.[8] The chemical makeup for the majority of materials used for the anode and electrolyte of lithium-ion batteries have progressively narrowed to structured graphite materials and lithium hexafluorophosphate ($LiPF_6$), respectively. This increased uniformity for the anode and electrolyte aid in the recyclability of lithium-ion batteries. However, this cannot be said for recent employed materials in cathodes. The concern is compounded, considering that the cathode contains the majority of precious metals found in lithium-ion batteries and is the primary target for recycling methods. While the industry predominately relied on lithium manganese oxide ($LiMn_2O_4$), denoted by LMO, and lithium cobalt oxide ($LiCoO_2$), denoted by LCO, in 1995, emerging materials have since been developed, broadening the distribution of common cathode applications. These advance materials, including lithium nickel manganese cobalt oxide ($LiNi_{⅓}Mn_{⅓}Co_{⅓}O_2$), denoted by NMC, lithium nickel cobalt aluminum oxide ($LiNi_{0.8}Co_{0.15}Al_{0.05}O_2$), denoted by NCA, and lithium iron phosphate ($LiFePO_4$), denoted by LFP, in addition to LMO and LCO, all rely on the ability for lithium ions to freely diffuse through the crystal structure.[8] The development of a variety of materials for cathode application is a result of economic considerations and resource availability.[8]

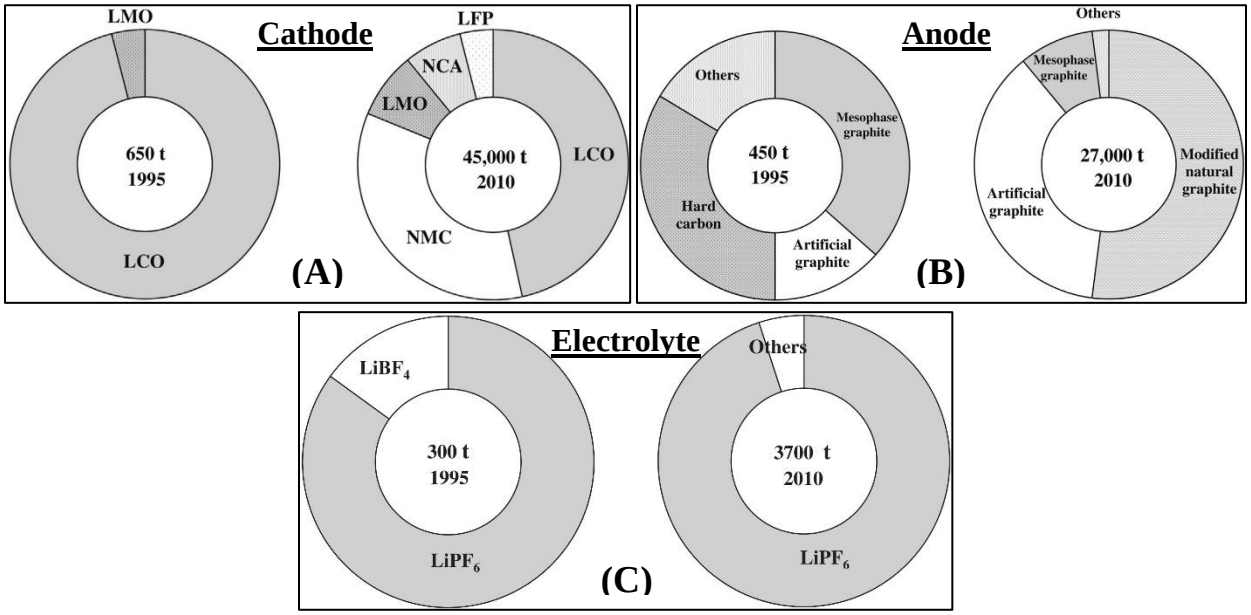

Figure 3. Comparison charts of the most common materials used for lithium-ion battery technologies in 1995 and 2010. **(A)** Comparison of materials used for the cathode, including LCO ($LiCoO_2$), LMO ($LiMn_2O_2$), NMC ($LiNi_{⅓}Mn_{⅓}Co_{⅓}O_2$), NCA ($LiNi_{0.8}Co_{0.15}Al_{0.05}O_2$), and LFP ($LiFePO_4$). **(B)** Comparison of materials used for the anode, including mesophase graphite, hard carbon, artificial graphite, modified natural graphite, and others. **(C)** Comparison of materials used for the electrolyte, including $LiPF_6$, $LiBF_4$, and others. [figure from Yoshino, A., Development of the Lithium-Ion Battery and Recent Technological Trends. In *Lithium-Ion Batteries*, Pistoia, G., Ed. Elsevier: Amsterdam, 2014; pp 1-20.]

An example of these considerations revolves around the availability of cobalt, which was a primary component in early lithium-ion battery technologies. The global supply of cobalt is estimated at 7 million metric tons, far less than that of lithium.[9] In addition to the scarcity of the resource, approximately 70% of the world's supply of cobalt is exported from Congo.[10] The Congo government, which has recently been scrutinized for unethical mining practices and unequal distribution of profits, has been unpredictable with corrupt electoral processes and minimal separation between corporation and political agendas.[11] This leads to uncertainty in the supply and potential volatility in the price for cobalt and has driven the development for alternative cathode materials that can use less or no cobalt.

Despite the various developed materials, lithium remains the common resource used in all forms of lithium battery technologies. It is important to distinguish the difference between lithium-ion and lithium-primary batteries. Lithium-ion batteries are typically rechargeable, relying on the diffusion of lithium ions between electrodes during the discharge and charging cycles.[12] Recycling of lithium-ion batteries remains of significant interest considering the expected surge in demand for their application in industries, such as electrified or electric cars as previously discussed. The electrolytes, primarily $LiPF_6$ used in lithium-ion battery cells, constitute significant safety considerations for their handling. The Global Harmonized System (GHS) for classification of hazards associated with chemicals considers $LiPF_6$ to be acutely toxic if inhaled, consumed, or in contact with skin or eyes.[13] It has also been determined that $LiPF_6$ can provide a mechanism to produce HF, an extremely acidic compound with high corrosivity and toxicity in minimal concentrations.[14, 15] Additionally, studies of $LiPF_6$ in common electrolyte solvents have shown to produce highly flammable gases, consisting of significant concentrations of hydrogen, ethane, propane, and pentane gas, when exposed to ambient air.[14] Thus, accidental puncture of lithium-ion cells can result in significant health, fire, and safety hazards. While lithium-ion batteries do not require lithium metal in their construction, its formation can occur during its lifetime through repeated cycles and various other environmental factors.

Alternatively, lithium primary batteries incorporate the use of lithium metal, or compounds containing lithium metal, as an electrode material. Lithium-primary batteries are not considered rechargeable which increases the need for effective recycling methods to recovery the lithium from consumed cells.[12] Handling of lithium metal and lithium metal compounds, however, involves significant safety considerations. Lithium metal is extremely reactive, with the ability to combust under the presence of oxygen, nitrogen, hydrogen, and carbon dioxide gas.[16] Lithium metal also reacts violently with water, producing caustic lithium hydroxide and spontaneously combustible hydrogen gas. Thus, direct exposure to air produces a significant fire and safety hazard and should be avoided.

Several disasters have occurred during the transportation of lithium-based batteries, with significant incidents outlined in **Table 2** below. Between 23 January 2006 and 22 January 2020, The Federal Aviation Administration (FAA) has cataloged 288 incidences associated with the transportation of lithium batteries by air alone.[17] As a result, the United States Department of Transportation (USDOT) categorizes lithium batteries as a class 9 shipping hazard and its transportation must abide by the federal regulation requirements, outlined by 49 CFR 173.185.

Date	Incident Description
4 January 2020	A Cosco Pacific shipping barge was traveling from Malaysia to India when a cargo container was reportedly engulfed in flames. The resulting fire destroyed two and damaged several surrounding containers. No personnel were injured during the incident and the containers were extinguished on site before being off loaded five days later. The cause of the fire was determined to be from a container carrying lithium batteries.
24 April 2017	A Union Pacific train car was transporting used lithium-ion batteries from the Port of New Orleans to a recycling center in San Antonio. Several batteries caught fire in one of the train cars in downtown Houston, resulting in an explosion. No personnel were injured, however, surrounding infrastructure was damaged from the explosion.
3 September 2010	A UPS 747 aircraft was transporting lithium batteries in the cargo hold when a fire was reported 22 minutes into the flight. Smoke bellowed into the aircraft cockpit, obscuring the visibility of the pilots. The plane crashed outside of Dubai, killing both crew members on board.
7 February 2006	A UPS DC8-71F aircraft was forced to conduct an emergency landing in Philadelphia after a fire broke out in the cargo hold. Flight members received immediate medical attention and no casualties were reported. The investigation suspected that the fire originated from goods containing lithium batteries.

Table 2. List of previous disasters associated with the transportation of lithium batteries.

These regulations impose significant costs for the transportation of lithium batteries and serves as another barrier to lithium battery recycling efforts. Significant research is currently being dedicated to developing methods which passivate the remaining active lithium in used lithium batteries.[18] During the lifetime of a lithium battery, passivation occurs on the surface of the electrodes resulting from repeated charge and/or discharge cycles. The characterization of the passivation layer formed depends on the chemistry used for the lithium battery. For most lithium-based battery technologies, the passivation layer primarily consists of lithium carbonate (Li_2CO_3) and lithium alkylcarbonates ($ROCO_2Li$).[19, 20] Historical incidences, however, have proven that used lithium batteries still contain significant amounts of active lithium compounds, as discussed above. OnTo Technology LLC, an advanced battery recycling company located in Bend, OR, has dedicated resources to developing a passivation method for used lithium batteries. Early development of their process involves pumping of liquid carbon dioxide into a used lithium battery cell, which serves the role of removing any remaining electrolyte solution from the electrodes in addition to passivating any remaining active lithium compounds.[21] While preliminary results are optimistic, further studies are required to confirm the absence of hazards associated with active lithium before shipping regulations for lithium batteries can be revised.

To aid in the advancement and confirmation of passivation methods for lithium batteries, an analytical technique for the quantification of active lithium compounds should be developed. This developed method can be used to confirm the absence or formation of free lithium metal in lithium-ion batteries. Additionally, it may also be used as proof for novel passivation techniques performed on lithium-primary batteries, such as the one developed by OnTo Technology discussed above. Current methods exist for identifying lithium content for a range of materials,

such as atomic emission spectroscopy (AES) and x-ray diffraction (XRD).[22] However, these methods involve high cost and sophisticated instruments that are not suitable for high throughput quantification of lithium. Supplemental techniques, such as nuclear magnetic resonance (NMR) spectroscopy, may also be required to differentiate between active and passivated lithium compounds. These spectrometers would require adaptations to handle active lithium compounds, resulting in significant costs and added impracticality for the emerging lithium battery recycling industry. Thus, the development of a safe, cost-effective, and robust chemical analysis technique for quantifying the amount of active lithium present in used lithium batteries was explored in this study.

One of the techniques evaluated involved a redox titration between active lithium and triiodide ions (I_3^-). The synthesis of I_3^- involves the combination of iodine (I_2) and an iodide salt, such as potassium iodide (KI) or sodium iodide (NaI), in a suitable solvent. Polyiodide compounds, such as I_3^-, undergo characteristic color changes when undergoing reductions, allowing for the use of ultraviolet-visible spectroscopy (UV/vis) to track the redox reaction. UV/vis spectroscopy serves as a robust and cost-effective analytical technique and would not require additional equipment for handling lithium, compared to AES and XRD, since the sample does not require ionization and is suspended in solution. Additionally, a back titration, using a thiosulfate ($S_2O_3^{2-}$) reductant, can also be used to correlate the amount of I_3^- reduced to the amount of active lithium originally added to the solution. It is also likely that the lithium compounds formed under passivation conditions, such as Li_2CO_3 and $ROCO_2Li$, as well as the common electrolyte solution, $LiPF_6$, will not react with I_3^-. While the overall reaction chemistry between lithium metal and I_3^- have been previously documented, this study further explores the kinetics involved and its feasibility for application in quantifying the amount of active lithium present in used lithium batteries.[23]

A second technique was also explored in addition to the redox titration method, involving pH titration. As previously stated, active lithium readily reacts with water to produce lithium hydroxide (LiOH) and hydrogen gas (H_2). The formation of the strong base, LiOH, can then be titrated using a strong acid, correlating the amount of titrant required for a neutral solution to the amount of active lithium originally present. A pH probe is a simple and cost-effective method for tracking the pH titration. Additionally, pH indicators, such as phenolphthalein, undergo characteristic color changes based on the acidity of the surrounding environment and can also be used to track the pH titration. However, there is uncertainty in this method surrounding the potential liberation of lithium from compounds associated with passivation, considering lithium's reactivity with water. This could result in an over-estimation of the remaining active lithium. To address these concerns, the pH titration method was also carried out by replacing water with methanol (MeOH) as the solvent system. Like the reaction above, the combination of lithium and MeOH results in the production H_2 gas and the strong base, lithium methoxide (CH_3OLi). It should be noted that the described pH titration above involves vigorous reactions with lithium and the production of spontaneously combustible H_2 gas, underscoring the need for safe laboratory practices.

Experimental.

1. Redox Titration of Lithium with Triiodide

a. Solvent Selection.

Organic solvents were selected and analyzed as candidates to carry out a redox titration technique. Each solvent was qualitatively studied for its ability to isolate, or solvate, active lithium metal while not dissolving lithium compounds associated with passivation. Each solvent was also analyzed for its ability to dissolve iodine and iodide salts, in addition to compounds that can serve as reducing agents for polyiodide compounds.

(i). Qualitative Experiments for Solubility of Various Solutes in Selected Solvents

Qualitative experiments were carried out on deionized water (H_2O), methanol (MeOH), n-butanol (n-BuOH), acetone, acetonitrile (ACN), and propylene carbonate (PC) to observe their solubilities with lithium metal ($Li_{(m)}$), sodium thiosulfate ($Na_2S_2O_3$), iodine (I_2), potassium iodide (KI), lithium iodide (LiI), and sodium iodide (NaI). A list of the reagents and their associated manufacturer and purities can be found in **Table 5** of **Supplemental Information 1**. This was performed by measuring out 5.0 mL of each solvent, using a 5-mL micropipette, into a 50-mL beaker placed on a stir plate. Using a pea-sized magnetic, Teflon stir bar, the solvents were stirred while slowly adding one of the specified solutes. Initial observations immediately after the solute addition, including color changes, the presence of solids, reaction activity, etc., were recorded. The solution was then allowed to sit overnight, recording any changes that occurred over time. Qualitative, experimental observations were then compared to literature reports to narrow down the list of potential solvents and iodide salts for use in a redox titration method.

b. Thiosulfate Back Titration.

Redox titration methods with triiodide (I_3^-) have been heavily utilized and studied in prior literature, especially using $Na_2S_2O_3$ as a reducing agent. The well-established redox reaction:

$$I_3^- + 2\,(S_2O_3)^{2-} \rightarrow 3\,I^- + (S_4O_6)^{2-} \quad \textbf{(1)}$$

was confirmed experimentally. In these experiments, $Na_2S_2O_3$ in DI H_2O for the titrant solution was titrated against a I_3^- solution prepared using I_2 and excess KI in acetonitrile. The required volume of titrant required to reach the endpoint indicating conversion of the colored I_3^- solution to a colorless I^- solution was recorded, and the volumetric ratio of titrant to analyte solution was also calculated to check for the effects of miscibility or solubility of the solutions.

(i). Synthesis of Thiosulfate Titrant Solution

The thiosulfate titrant solution was synthesized by combining 0.1580 g ($9.993 \cdot 10^{-4}$ mol) of $Na_2S_2O_3$ in a 100-mL volumetric flask with DI H_2O to produce a 100.0 mL $9.993 \cdot 10^{-3}$ M solution. The solution was mixed, using the head-over-end method, until no solids were visible. The aqueous thiosulfate solution was carefully added to a 50-mL graduated burette, and a small

amount of solution was poured out to ensure the burette tip was absent of all air bubbles before recording the initial volume.

(ii). Synthesis of Triiodide Solution

The I_3^- solution was synthesized by combining 0.0253 g ($9.968 \cdot 10^{-5}$ mol) of I_2, 0.0849 g ($5.114 \cdot 10^{-5}$ mol) of excess KI, and ACN in a 100-mL volumetric flask to produce a 100.0 mL $9.968 \cdot 10^{-4}$ M solution. Approximately 50 mL of the ACN solvent was poured into the volumetric flask prior to adding the I_2 and then KI solutes. The volumetric flask was continuously stirred and agitated during the addition of the remaining ACN solvent before performing the head-over-end method to ensure a well-mixed solution with no solids present.

(iii). Thiosulfate-Triiodide Titration Procedure

Using a 10-mL volumetric pipette, a 10.0 mL sample of the well-mixed triiodide solution was poured into a 50-mL flask along with a pea-sized magnetic, Teflon stir bar. The flask was then placed on a stir plate positioned directly under the tip of the burette containing the aqueous thiosulfate titrant solution. The tip of the burette was position slightly above the surface level of the triiodide solution to ensure minimal splashing while avoiding contamination of the tip with the titrating solution. The triiodide solution was then titrated with the aqueous thiosulfate titrant until the solution became colorless, indicating that all I_3^- ions have been reduced to iodide ions. This procedure was replicated in triplicate.

c. UV/vis Analysis for Triiodide Concentration

An important characteristic of polyiodide compounds, which make their uses favorable for quantitative redox reactions, are the characteristic color changes that occur during their reduction and oxidation. In a study conducted by Wei, et al, two characteristic peaks in the UV/vis spectrum for I_3^- occur at 288 and 350 nm.[24] This was confirmed in this work by synthesizing several different dilutions of I_3^- in PC and performing UV/vis analysis to define the operable range where these two characteristic peaks can be observed with good resolution.

(i). Synthesis of Triiodide Solution at Various Dilutions

I_3^- solutions were synthesized by first combining 0.0127 g ($5.000 \cdot 10^{-5}$ mol) of I_2, 0.0335 g ($2.500 \cdot 10^{-4}$ mol) of excess LiI, and PC in a 50-mL volumetric flask to produce a 50.0 mL$1.000 \cdot 10^{-3}$ M solution. Approximately 25 mL of PC was poured into the volumetric flask prior to adding the I_2 and then LiI solutes. The volumetric flask was continuously stirred and agitated during the addition of the remaining PC before performing the head-over-end method to ensure a well-mixed solution with no solids present. Using a 5-mL micropipette, 5.0 mL of the previously synthesized I_3^- solution was transferred to a separate 50-mL volumetric flask and combined with PC to produce a 50.0 mL $1.00 \cdot 10^{-4}$ M I_3^- solution. This procedure was repeated to produce $1.00 \cdot 10^{-5}$ M and $1.00 \cdot 10^{-6}$ M I_3^- solutions.

(ii). UV/vis Analysis of Triiodide Solutions

A 5-mL two-sided, quartz cuvette was used to analyze the I_3^- solution for UV/vis spectroscopy. The quartz cuvette was initially washed with ethanol (EtOH) and allowed to dry

before washing again with PC. A glass pipette was then used to add pure PC to the cuvette, which served as calibration standard for the UV/vis spectrometer. Once again, the cuvette was washed with ethanol and allowed to dry before washing again with the first dilution, $1.00 \cdot 10^{-3}$ M, of I_3^- solution. A separate glass pipette was then used to add the first I_3^- dilution to the washed cuvette, which was analyzed using the calibrated UV/vis spectrometer. This procedure was repeated to analyze the $1.00 \cdot 10^{-4}$ M, $1.00 \cdot 10^{-5}$ M, and $1.00 \cdot 10^{-6}$ M I_3^- dilutions.

d. Triiodide Stability in Selected Solvents

Although the overall reaction chemistry of $Li_{(m)}$ and I_3^- is well known:

$$2\ Li_{(m)} + I_3^- \rightarrow 2\ Li^+ + 3\ I^- \quad \textbf{(2)}$$

the reaction mechanism has not been reported. With the reaction mechanism and kinetics unknown, it is critical to understand the stability of I_3^- in the candidate solvents to be tested for the proposed redox titration. The stability of I_3^- in ACN and PC were also analyzed, recording hourly and daily UV/vis measurements of I_3^- solutions stored both in and in the absence of light. Copper metal ($Cu_{(m)}$) foil is a common anode current collector in lithium-ion batteries and serves as a potential competitive reductant in the proposed redox titration method for used lithium-ion cells. Thus, the reaction of $Cu_{(m)}$ with I_3^- was studied here, alongside stability experiments.

(i.) Short-Term Triiodide Stability

Using the synthetic procedures described above, 50.0 mL of $1.00 \cdot 10^{-4}$ M I_3^- was synthesized in PC. Taking a 5-mL two-sided, quartz cuvette, a pure sample of PC was added to the cuvette, which served as the calibration standard for the UV/vis spectrometer. Again, following the UV/vis analysis procedures described above, the synthesized I_3^- solution was analyzed for its short-term stability using the calibrated UV/vis spectrometer. Samples were tested at 30, 60, 90, 120, 150, 180, 210, 240, and 300 minutes after synthesis.

(ii.) Long-Term Triiodide Stability and Reactivity with Copper Metal

Using the synthetic procedures described above, 50.0 mL of $1.00 \cdot 10^{-4}$ M I_3^- was synthesized in ACN. This solution was then evenly divided between two 20-mL, glass sample vials. A 0.0215 g sample of copper foil was added to one of the vials and stored alongside the second vial in the absence of light. The synthesized I_3^- solution in PC used in the ‘Short-Term Triiodide Stability’ experiment was then evenly divided between three 20-mL, glass sample vials. A 0.0215 g sample of copper foil was added to one of the vials and stored alongside a second vial in the absence of light. The third vial was stored near a window with direct access to both indoor lighting and sunlight. Samples were taken from each of the stored vials and analyzed under UV/vis spectroscopy, following the procedures described above. The UV/vis spectrometer was calibrated each time with a pure sample of ACN or PC, depending on the analyte being tested. Samples from each vial were tested for its long-term stability at 1, 2, 3, 4, 5, 6, 8, and 11 days after its initial synthesis.

e. Redox Titration Method for Reduction of Triiodide via Lithium Metal

The proposed redox titration method for the reduction of I_3^- by unpassivated $Li_{(m)}$ remaining in a used, lithium-ion cell was explored. Due to the high reactivity of $Li_{(m)}$ in the presence of oxygen (O_2) gas and H_2O, reagents necessary to produce the I_3^- analyte solution for the titration were dried prior to use. Since any remaining, active lithium should react with I_3^- once placed in the analyte solution, the titrant solution can be synthesized under standard atmospheric conditions. Using the same reasoning, the titration method can also be carried out under standard atmospheric conditions without the concern for O_2 or H_2O interference. A proof of concept experiment was also conducted, using excess $Li_{(m)}$, to test the proposed redox reaction.

(i.) Preparation of Iodine

The reagents necessary to synthesize the I_3^- analyte solution, solid LiI and I_2, were dried prior to synthesis and the addition of $Li_{(m)}$. I_2 was placed in a 20-mL sealable, glass test tube, which was then sealed and positioned on a hot plate, ensuring contact between the bottom of the tube and the top of the hot plate. The hot plate was set to 30 °C, allowing the I_2 to sublime and recrystallize on the sides of the vial overnight.

(ii.) Preparation of Lithium Iodide

To dry the LiI reagent, it was placed into a 20-mL sample vial, which was then covered with aluminum foil with small holes to allow for pressurization and depressurization. The covered sample vial was placed into a vacuum oven and heated to 60 °C under vacuum for 1 h. The sample was then heated to 120 °C under vacuum for an additional hour.

(iii.) Proof of Concept Test with excess Lithium Metal

Using a 50-mL volumetric flask, 0.0075 g ($5.600 \cdot 10^{-5}$ mol) of dried LiI was added to be used for synthesizing a concentrated LiI solution. The volumetric flask containing LiI was then carefully transferred to an Ar-purged glovebox and combined with anhydrous PC to produce a 50.0 mL $3.90 \cdot 10^{-3}$ M I^- solution. Taking a 100-mL volumetric flask, 0.04958 g ($1.950 \cdot 10^{-4}$ mol) of dried I_2 was added along with approximately 10 mL of anhydrous PC. This was quickly performed before carefully transferring the volumetric flask containing I_2 in PC to the Ar-purged glovebox. It is important to note that this step is necessary to avoid the sublimation of I_2 at room-temperature – opening solid I_2 inside a glovebox may potentially contaminate the controlled atmosphere. Using a 5-mL micropipette, 2.5 mL of the previously synthesized $3.90 \cdot 10^{-3}$ LiI solution was added to the 100-mL volumetric flask containing I_2 in PC. The remaining volume of the 100-mL volumetric flask was then filled with anhydrous PC to produce a 100.0 mL $9.75 \cdot 10^{-5}$ M I_3^- solution. Continuing work in the glovebox, 15.0 mL samples of the synthesized I_3^- solution was added to two 20-mL glass sample vials, using a 5-mL micropipette in 5.0 mL increments. A small piece of $Li_{(m)}$, approximately 5x5x0.45 mm, was then placed in one of the samples before sealing both vials and removing from the glovebox. The samples were then analyzed, following the UV/vis analysis procedures described above, at initial synthesis and

again after one day and one month. Both samples were stored in the Ar-purged glovebox in between UV/vis measurements.

2. pH Titration of Lithium with a Strong Acid

a. pH Method Development in Water

Although the overall reaction chemistry of $Li_{(m)}$ and H_2O is well known:

$$2Li_{(m)} + 2H_2O_{(l)} \rightarrow 2LiOH_{(aq)} + H_{2(g)} \quad \textbf{(3)}$$

the use of this reaction to quantify the amount of active lithium, specifically in used lithium-ion cells, have not been reported. The described reaction results in the generation of a stoichiometric amount hydroxide ions (OH^-) to the amount of $Li_{(m)}$ added. Thus, the resulting basic solution can be titrated using a strong acid, correlating the amount of titrant required to bring the solution to a neutral pH to the amount of $Li_{(m)}$ added. For this experiment, sulfuric acid (H_2SO_4) served as the strong acid titrant:

$$2LiOH_{(aq)} + H_2SO_{4(aq)} \rightarrow Li_2SO_{4(aq)} + 2H_2O_{(l)} \quad \textbf{(4)}$$

resulting in a 2:1 stoichiometric ratio for lithium hydroxide (LiOH) and H_2SO_4, respectively. To allow for the experiment to take place under standard atmospheric conditions, solid lithium hydroxide (LiOH) was used in place of $Li_{(m)}$. The reaction above was then confirmed, titrating various dilutions of LiOH in DI H_2O to produce a standard curve relating the molarity of the LiOH to the required volume of titrant. To monitor the pH of the solution during titration, a phenolphthalein (phph) indicator was used, which turns a bright pink color in basic solutions and becomes colorless in acidic solutions. Thus, it is necessary to take caution when nearing the endpoint to avoid over titrating and creating an acidic solution. A list of the reagents and their associated manufacturer and purities can be found in **Table 6** of **Supplemental Information 1**.

(i.) Synthesis of Sulfuric Acid Titrant Solution

The sulfuric acid titrant solution was synthesized using a 1-mL volumetric pipette to measure out 1.00 mL ($1.88 \cdot 10^{-2}$ mol) of H_2SO_4 in a 250-mL volumetric flask with DI H_2O to produce a 100 mL $7.50 \cdot 10^{-2}$ M solution. The aqueous H_2SO_4 solution was carefully added to a 50-mL graduated burette, and a small amount of solution was poured out to ensure the burette tip was absent of all air bubbles before recording the initial volume.

(ii.) Synthesis of Lithium Hydroxide Solution

The LiOH solution was synthesized by combining 0.4754 ($1.985 \cdot 10^{-2}$ mol) of LiOH and DI H_2O in a 100-mL volumetric flask to produce a 100.0 mL $1.985 \cdot 10^{-1}$ M solution. The solution was mixed, using the head-over-end method, until no solids were visible.

(iii.) pH Titration in Water Procedures at Various Lithium Hydroxide Dilutions

Using a 5-mL volumetric pipette, 5.0 mL of the $1.985 \cdot 10^{-1}$ M LiOH solution was transferred to a 20-mL glass sample vial with a pea-sized magnetic, Teflon stir-bar. One drop of phph indicator was then added to the vial, which was placed on a stir plate positioned directly

under the tip of the burette containing the aqueous H_2SO_4 titrant solution. The tip of the burette was position slightly above the surface level of the triiodide solution to ensure minimal splashing while avoiding contamination of the tip with the titrating solution. The LiOH solution was then titrated until the solution just starts to become colorless. A $1.6 \cdot 10^{-1}$ M LiOH solution was then synthesized, using a 4-mL and 1-mL volumetric pipette to combine 4.0 mL and 1.0 mL of $1.985 \cdot 10^{-1}$ M LiOH solution and DI H_2O in a 20-mL glass vial, respectively. This solution was then titrated using the same procedures described above. The above procedures were used to titrate $1.2 \cdot 10^{-1}$ M, $7.9 \cdot 10^{-2}$ M, and $4.0 \cdot 10^{-2}$ M LiOH solutions. This entire procedure was replicated in triplicate for each LiOH dilution.

b. pH Method Development in Methanol

To quantify the remaining, active lithium contained in used lithium-ion cells, it is imperative that compounds associated lithium passivation be negated during the quantification method. In terms of the pH titration, passivated lithium compounds should not dissolve in the analyte solution. Thus, an alternative pH method was explored, replacing DI H_2O with MeOH as the lithium hydroxide solvent resulting in different analyte solubilities. Although the overall reaction chemistry of Li(m) and MeOH is well known:

$$2Li_{(m)} + 2CH_3OH_{(l)} \rightarrow 2CH_3OLi_{(l)} + H_{2(g)} \quad \textbf{(5)}$$

the use of this reaction to quantify the amount of active lithium, specifically in used lithium-ion cells, have not been reported. The described reaction results in the generation of a stoichiometric amount methoxide ions (CH_3O^-) to the amount of $Li_{(m)}$ added. Similar to the pH titration in DI H_2O, the resulting basic solution can be titrated using a strong acid, correlating the amount of titrant required to bring the solution to a neutral pH to the amount of $Li_{(m)}$ added. Once again, sulfuric acid (H_2SO_4) served as the strong acid titrant:

$$2CH_3OLi_{(l)} + H_2SO_{4(aq)} \rightarrow Li_2SO_{4(aq)} + 2CH_3OH_{(l)} \quad \textbf{(6)}$$

resulting in a 2:1 stoichiometric ratio for lithium methoxide (CH_3Li) and H_2SO_4, respectively. The same methodology used in the pH titration was also used for this experiment, thus the titrant and analyte synthesis, along with the titration procedures, are not repeated here.

Results & Discussion.

1. Redox Titration of Lithium with Triiodide

a. Solvent Selection.

For the redox titration method, any remaining active $Li_{(m)}$ in the used lithium-ion battery cell I_3^- is reduced to I^- according to:

$$2\ Li_{(m)} + I_3^- \rightarrow 2\ Li^+ + 3\ I^- \quad \textbf{(2)}$$

Therefore, the solvent used in the titration must dissolve the required reagents but not interfere with this reaction, and not compromise the passivation layer developed by the reductant, $Li_{(m)}$. Ideally, the same solvent would be employed to synthesize I_3^- from the reaction between I_2 and an iodide salt, in this case the solvent must also dissolve these reagents. Finally, since the method to quantify the residual I_3^- requires back titration with a thiosulfate ($S_2O_3^{2-}$) solution:

$$I_3^- + 2\,(S_2O_3)^{2-} \rightarrow 3\,I^- + (S_4O_6)^{2-} \qquad \textbf{(1)}$$

the solvent should also dissolve $Na_2S_2O_3$ or be miscible with a thiosulfate solution.

Solvent	Reactivity w/ $Li_{(m)}$	Solubility of I_2	Solubility of KI	Solubility of LiI	Solubility of NaI	Solubility of $Na_2S_2O_3^{2-}$
Water (DI H_2O)	Highly Reactive	Slightly Soluble	Highly Soluble	Highly Soluble	Highly Soluble	Highly Soluble
Methanol (MeOH)	Highly Reactive	Not Soluble	Highly Soluble	Highly Soluble	Highly Soluble	Not Soluble
n-Butanol (n-BuOH)	Slightly Reactive	Slightly Soluble	Not Soluble	Highly Soluble	Highly Soluble	Not Soluble
Acetone	Moderately Reactive	Not Soluble	Slightly Soluble	Highly Soluble	Highly Soluble	Not Soluble
Acetonitrile (ACN)	Not Reactive	Highly Soluble	Slightly Soluble	Highly Soluble	Highly Soluble	Not Soluble
Propylene Carbonate (PC)	Not Reactive	Slightly Soluble	Slightly Soluble	Slightly Soluble	Slightly Soluble	Not Soluble

Table 3. Solubility and reactivity of organic solvent candidates for the redox titration experiment. Solvents were evaluated for both the triiodide and thiosulfate titrations.

From **Table 3** shown above, ACN and PC were the best candidates for the I_3^- analyte solution due to their minimal reactivity with $Li_{(m)}$. Additionally, both ACN and PC are good solvents for iodine and iodide salts, with ACN having a high solubility for LiI and NaI. Thus, both solvents were further evaluated for the I_3^- analyte solution during the redox titration analysis.

DI H_2O was determined to be the only candidate capable of solvating $Na_2S_2O_3$, as shown in **Table 3** above. While it is not critical for the titrant solvent to be inert with $Li_{(m)}$ and soluble with I_3^- compounds, it must be miscible with the solvents used for the I_3^- analyte solution to allow for the interaction between $S_2O_3^{2-}$ and I_3^-. Fortunately, DI H_2O is considered completely miscible with ACN.[25] While PC is not completely miscible with DI H_2O, it is highly soluble, capable of 175 g/L.[26] Thus, DI H_2O was selected for the $S_2O_3^{2-}$ titrant solution during the redox titration analysis.

b. Thiosulfate Back Titration.

Redox titration methods with I_3^- have been widely studied in prior literature, using $S_2O_3^{2-}$ as a reducing agent. The well-established redox reaction, shown in Equation (2), will be utilized in the proposed redox titration method to quantify the amount of I_3^- reduced by $Li_{(m)}$ in a back titration.[27] The 2:1 stoichiometric ratio between $S_2O_3^{2-}$ and I_3^- in the reaction above was confirmed for the selected solvent system, titrating samples of I_3^- in ACN with a $S_2O_3^{2-}$ titrant in DI H_2O.

	Volume of Triiodide Solution [mL]	Theoretical Volume of Titrant Required [mL]	Experimental Volume of Titrant Required [mL]
Sample #1	10.0	1.99	1.99
Sample #2	10.0	1.99	1.96
Sample #3	10.0	1.99	1.97

Table 4. Thiosulfate back titration test with $9.968 \cdot 10^{-4}$ M triiodide analyte solution in ACN and $9.993 \cdot 10^{-3}$ M thiosulfate titrant solution in DI H_2O.

From **Table 4** above, the average volume required to titrate the 10.0 mL I_3^- analyte samples in ACN was 1.97 ± 0.02 mL of $S_2O_3^{2-}$ titrant solution in DI H_2O. The observed molar ratios were therefore 1% below the theoretical stoichiometry of 2:1 $S_2O_3^{2-}$ to I_3^-. At the I_3^- concentration used above, this results in a maximum error of $1.97 \cdot 10^{-6}$ mol of I_3^-, which corresponds to only $2.75 \cdot 10^{-5}$ g of $Li_{(m)}$ when applied to the proposed I_3^- and $Li_{(m)}$ redox reaction, shown in **Equation (1)**. This confirms that the selected solvent system is sufficient for conducting the I_3^- and $S_2O_3^{2-}$ redox reaction with an error consistent with previous studies when performing the titration under room light.[27] One reasonable explanation for the difference between the theoretical and experimental volume of titrant required may using an inaccurate I_3^- concentration from the synthesis via I_2 and KI. As shown in **Table 3**, KI was observed to be only slightly soluble in ACN. While KI was added in excess to I_2, if not enough KI dissolved to react with all the I_2, the I_3^- concentration would be lower than expected resulting in a decreased amount of $S_2O_3^{2-}$ titrant required. A second explanation, which is discussed in previous literature, is the liberation of I_2 during titrations carried out in ambient light.[27] If the I_3^- solution was not immediately titrated upon synthesis in the absence of light, an error of 1.7% below the expected $S_2O_3^{2-}$ concentration was obtained.[27]

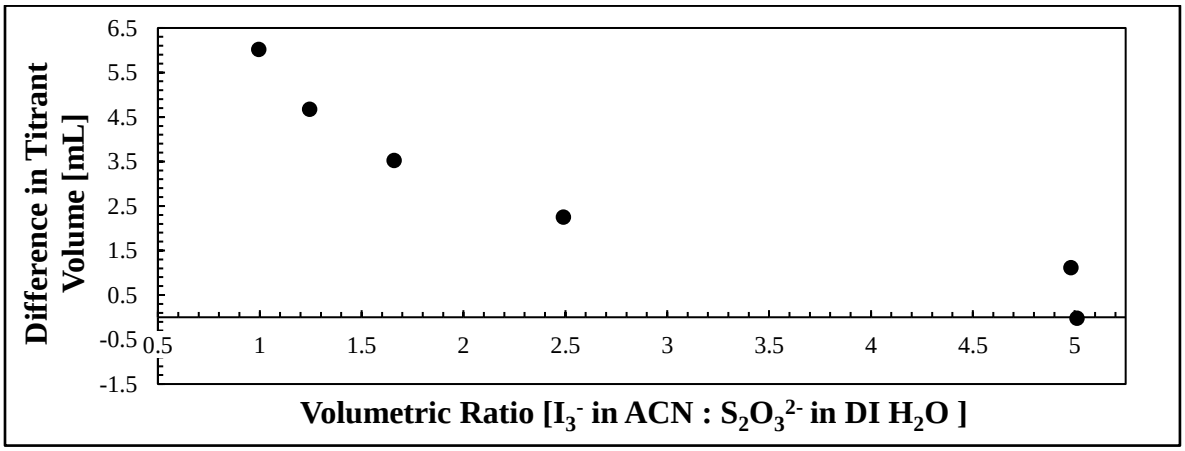

Figure 4. Graph of the difference between the expected, theoretical volume and the experimental volume of $S_2O_3^{2-}$ titrant required versus the volumetric ratio between I_3^- in ACN and $S_2O_3^{2-}$ in DI H_2O, respectively.

It should also be noted that the relative concentrations of I_3^- and $S_2O_3^{2-}$ solutions, and consequently the volumetric ratio of titrant to sample, were correlated to the deviation from theoretical stoichiometry of the reaction. As shown in **Figure 4**, a ~5:1 volumetric ratio between the ACN analyte and DI H_2O titrant solution, respectively, was determined to consistently result in the expected 2:1 stoichiometric ratio for $S_2O_3^{2-}$ to I_3^-. This study was performed as a result of

significant experimental discrepancy from the theoretical stoichiometry during initial titrations between $S_2O_3^{2-}$ and I_3^-, which is not explained by the sources of error proposed above. The low solubility of I_2 in DI H_2O, with a value of just 0.330 g/L at 25 °C, may have caused the reagent to precipitate from the ACN analyte solution during the titration.[28] The combination of aqueous I_2 in the presence of I_3^- and excess I^- at 25 °C has been reported to form larger polyiodide chains, such as I_5^- and I_6^{2-}, which would impact the stoichiometry of required $S_2O_3^{2-}$ titrant.[29] The determination of the exact cause of error in these titrations was deemed beyond the scope of this study and not investigated further.

c. UV/vis Analysis for Triiodide Concentration

An important characteristic of polyiodide compounds, which make their use favorable for quantitative redox reactions, is a characteristic color change from deep red/orange to colorless upon reduction to iodide. Thus, an additional method for tracking the reduction of I_3^- to I^- can be use of UV/vis spectroscopy to correlate the intensity of the characteristic I_3^- peaks, at 288 and 350 nm, to the concentration of I_3^- in the analyzed sample.[24] However, since I_3^- forms very deeply colored solutions, they can only be quantitatively analyzed at low concentration.

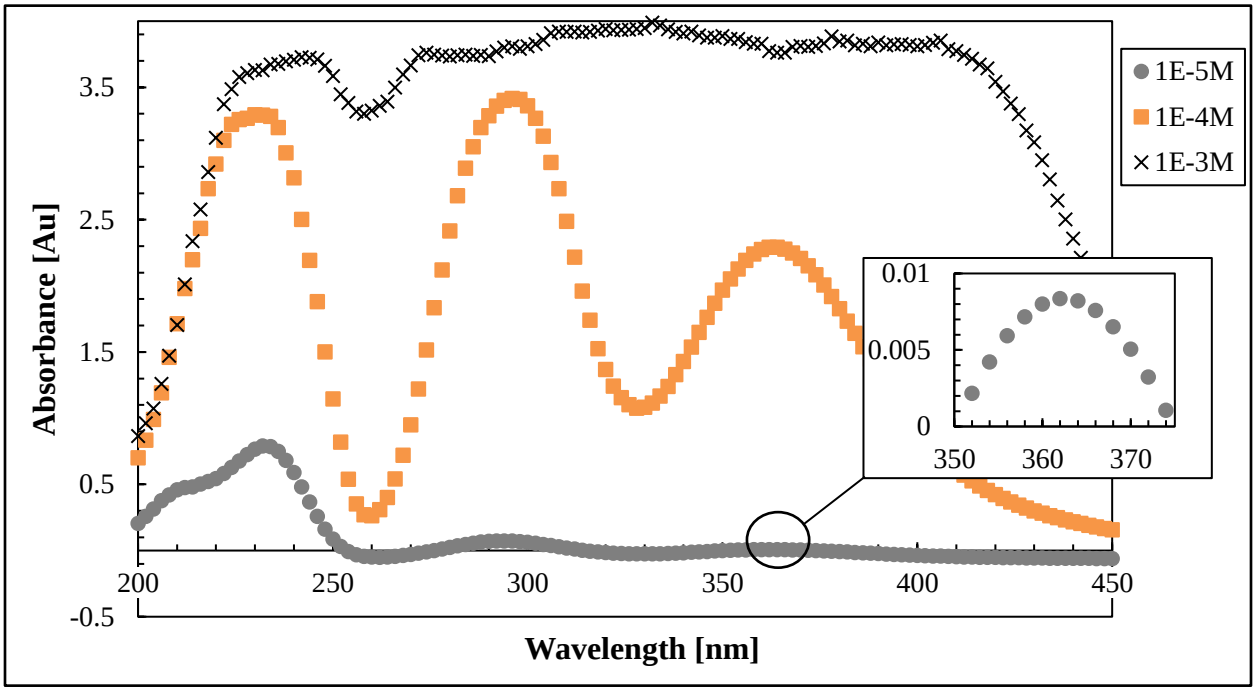

Figure 5. UV/vis spectroscopy results of $1.000 \cdot 10^{-3}$ M (black 'x'), $1.00 \cdot 10^{-4}$ M (orange '□'), and $1.00 \cdot 10^{-5}$ M (grey '○') I_3^- solutions in PC. Absorbance of ~4 represents the UV/vis detector is out of range for quantification.

From **Figure 5** above, the operable, UV/vis concentration range for I_3^- lies between ~10^{-4} and ~10^{-5} M, with the I_3^- concentration of $1.000 \cdot 10^{-3}$ M maxing out the UV/vis detector. The maximum intensity of the first characteristic I_3^- peak, around ~288 nm, was determined to be 3.42 au and 0.0742 au for $1.00 \cdot 10^{-4}$ M and $1.00 \cdot 10^{-5}$ M I_3^- solutions, respectively. The maximum intensity of the second characteristic I_3^- peak, around ~350 nm, was determined to be 2.29 au and 0.00836 au for $1.00 \cdot 10^{-4}$ M and $1.00 \cdot 10^{-5}$ M I_3^- solutions, respectively. It should be noted that a registered absorption of ~4 au represents the UV/vis detector has reached its

maximum allowable absorption. Thus, caution should be used when evaluating I_3^- concentration above 10^{-4} M, where absorption values are close to ~4 au, to avoid effects when nearing the limitation of the UV/vis detector. Similarly, caution should be used when analyzing I_3^- concentrations below 10^{-5} M, for extremely low absorption values, near the limitations of the UV/vis detector, are less accurate and vulnerable to trace contaminants.

It should also be noted that the maximum intensity of the characteristic I_3^- peaks were slightly shifted from the posted literature values of 288 and 350 nm.[24] The first characteristic I_3^- peak displayed absorbance maxima at 296 nm and 294 nm, with the second characteristic peak centered at 364 nm and 362 nm, for the $1.00 \cdot 10^{-4}$ M and $1.00 \cdot 10^{-5}$ M I_3^- samples, respectively. These small frequency shifts in the observed I_3^- peaks can be attributed to solvent effects, where I_3^- was analyzed using an aqueous system for the posted literature values has been compared to using I_3^- in PC for the above experiment.[24]

d. Triiodide Stability in Selected Solvents

Although the overall reaction chemistry of $Li_{(m)}$ and I_3^- is well documented, the reaction mechanism has not been reported.[23] With the reaction mechanism and kinetics unknown, it is critical to understand the stability of I_3^- in the candidate solvents and in the presence of potential contaminants found in lithium-ion battery cells. A practical quantitative method for determining the amount of active $Li_{(m)}$ in a used battery cell would ideally give results in the shortest amount of time possible. However, if the kinetics for the reduction of I_3^- to I^- by $Li_{(m)}$ proves slow, it is important to understand the natural degradation of I_3^- in the candidate solvent systems in different environments. Thus, both short and long-term stability experiments were conducted for I_3^- solutions.

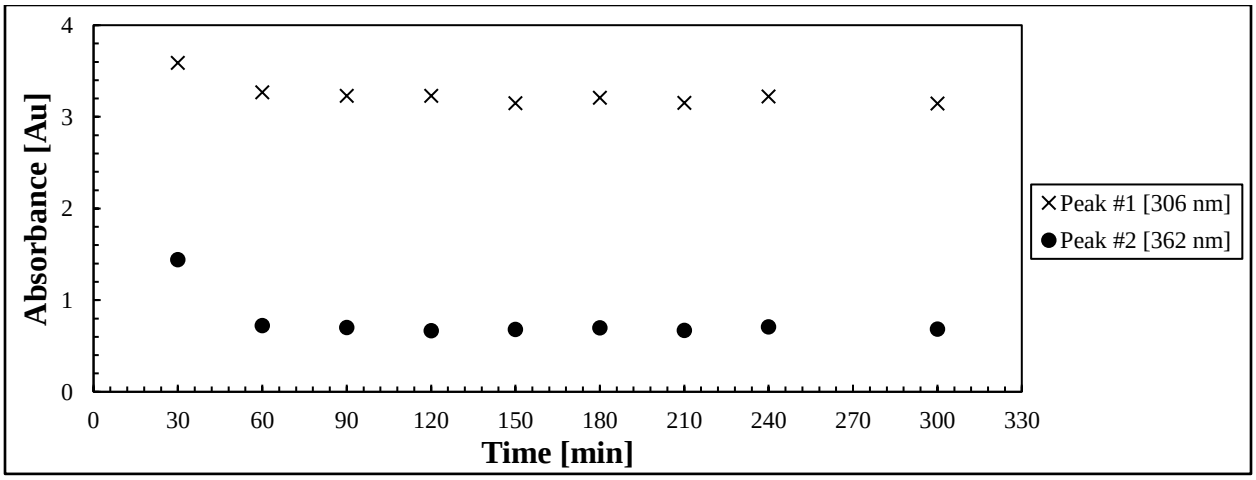

Figure 6. UV/vis spectroscopy results of the maximum intensity for the first (black 'x') and second (black '○') characteristic I_3^- peaks over time in the short-term (min). The analyte solution consisted of $1.00 \cdot 10^{-4}$ M I_3^- in PC stored under ambient conditions and lighting.

The short-term stability analysis of I_3^- in PC, as shown in **Figure 6** above, resulted in an immediate drop in absorbance for the characteristic peaks 60 min after synthesis. Between 60 min and 300 min after synthesis, the characteristic I_3^- peaks remained relatively stable in

intensity, with an average absorbance of 3.20 ± 0.05 au and 0.69 ± 0.02 au for the first and second characteristic peak, respectively. Thus, the redox titration method should allow more than 60 mins after the initial synthesis of the I_3^- solution before introducing the $Li_{(m)}$ sample to ensure that the I_3^- absorbance is stable. Introducing a $Li_{(m)}$, or used lithium-ion battery, sample to the I_3^- solution too early after synthesis would lead to an inaccurate quantification of the active $Li_{(m)}$, with an error as large as 0.77 au or 110%.

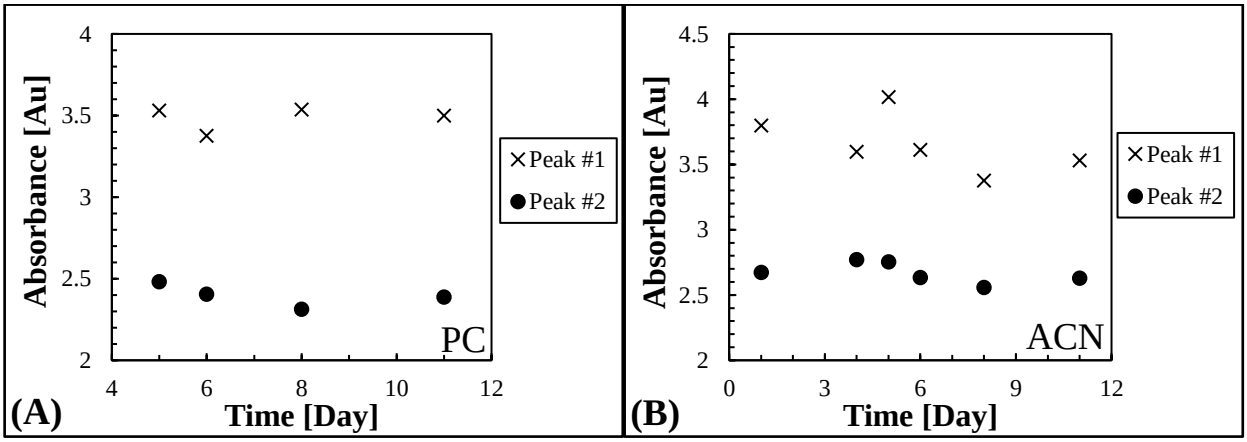

Figure 7. UV/vis spectroscopy data showing the maximum intensity for the first (black 'x') and second (black '○') characteristic I_3^- peaks over time in the long-term (days). **(A)** The analyte solution consisted of $1.00 \cdot 10^{-4}$ M I_3^- in PC stored in atmospheric conditions in the absence of light in between samples. **(B)** The analyte solution consisted of $1.00 \cdot 10^{-4}$ M I_3^- in ACN stored in atmospheric conditions in the absence of light in between samples.

The long-term stability of I_3^-, shown above in **Figure 7**, resulted in a relatively stable concentrations for both the PC, in **Figure 7A**, and the ACN, in **Figure 7B**, solvent systems, with slight decay trends beginning on day five. The PC and ACN I_3^- stability tests were conducted in parallel, testing the $1.00 \cdot 10^{-4}$ M I_3^- in ACN and the $1.00 \cdot 10^{-4}$ M I_3^- in PC samples. During this time, the UV/vis spectrometer, at OSU's integrated laboratory, was experiencing technical issues revolving around the ignition of the ultraviolet and visible light sources. Reliable data were obtained after initial ignition; however, they became more variable over time, resulting in poorer resolution and analysis for the PC samples. During the latter half of this stability experiment, the UV/vis spectrometer had been repaired, resulting in more consistent performance. Thus, UV/vis results obtained through day four were omitted from **Figure 7**. Replicate data should have been obtained, if more time and a larger volume of synthesized I_3^- analyte solutions were available.

The UV/vis data for the PC solvent system resulted in relatively consistent maximum intensities, with an average absorbance of 3.49 ± 0.08 au and 2.40 ± 0.07 au for the first and second characteristic I_3^- peaks, respectively. The UV/vis results for the ACN solvent system possess an outlier on day two, where the second characteristic I_3^- peak displayed a maximum intensity at a wavelength inconsistent with the other data points, at 350 nm compared to 362 ± 1 nm, respectively. This inconsistency was also attributed to the technical issues with the UV/vis spectrometer, and these data were omitted from **Figure 7B**. The I_3^- samples in ACN similarly resulted in relatively consistent maximum intensities, with an average absorbance of 3.7 ± 0.2 au and 2.67 ± 0.08 au for the first and second characteristic I_3^- peaks, respectively. Thus, it can be concluded that the concentration of I_3^- for both solvent systems is stable over long periods of

time. Further testing is recommended to confirm this result, employing a larger volume of I_3^- analyte solutions at a lower concentration, closer to ~$5 \cdot 10^{-5}$ M, to allow for replicate sampling and to avoid undesired effects when nearing the maximum limitation of the UV/vis detector, respectively.

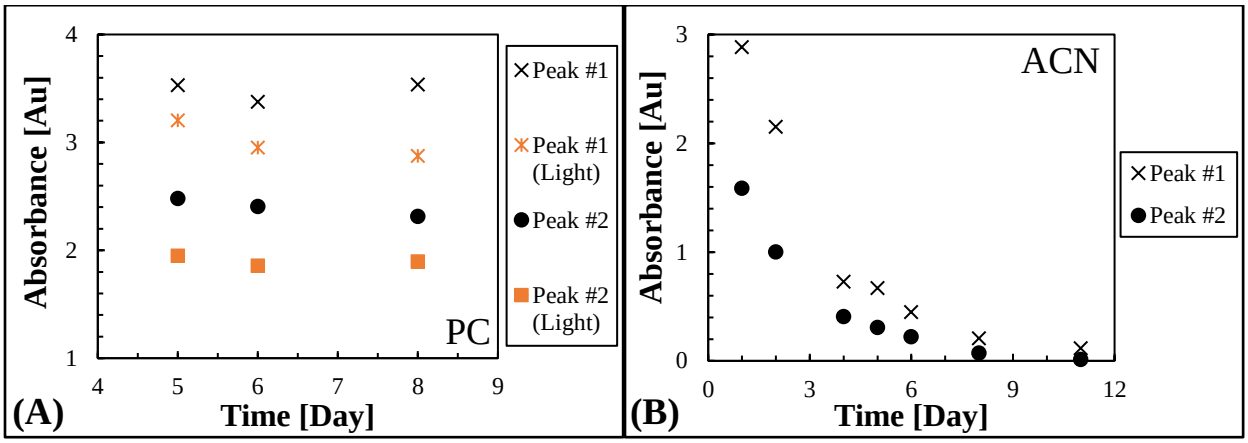

Figure 8. UV/vis spectroscopy results of the maximum intensity for the first and second characteristic I_3^- peaks over time in the long-term (days). **(A)** The analyte solution consisted of $1.00 \cdot 10^{-4}$ M I_3^- in PC stored in atmospheric conditions. The plot includes a data set for the first (black 'x') and second (black '○') characteristic I_3^- peaks in the absence of light along with data set for the first (orange '*') and second (orange '□') characteristic I_3^- peaks in the presence of both sun and laboratory lighting in between samples. **(B)** The analyte solution consisted of $1.00 \cdot 10^{-4}$ M I_3^- in ACN containing a copper foil sample stored in atmospheric conditions in the absence of light in between samples.

Additional factors, which may affect the overall stability of I_3^- in solution, were also considered during the long-term stability experiments. Shown in **Figure 8A** above, a comparison study was performed, storing the $1.00 \cdot 10^{-4}$ M I_3^- in PC sample both in and in the absence of light. The results from **Figure 8A** show similarities in the general trend for I_3^- samples stored in light and in darkness with the overall concentration of I_3^- remaining relatively stable over a long period of time. However, the sample exposed to light consistently showed lower maximum intensities for both the first and second characteristic I_3^- peaks. The I_3^- samples stored in light was on average 0.5± 0.2 au and 0.50 ± 0.07 au less than the I_3^- samples stored in darkness.

As previously discussed, $Cu_{(m)}$ is a common material used for the anode current collector and poses as a potential competitive reductant in the proposed redox titration method for used lithium-ion batteries. Thus, a 0.0215 g $Cu_{(m)}$ foil sample was added to a $1.00 \cdot 10^{-4}$ M I_3^- ACN solution, stored in darkness between sampling, to observe the long-term stability of I_3^- when exposed to $Cu_{(m)}$. The results, as shown in **Figure 8B** above, clearly show an exponential decay in the maximum intensities for both characteristic I_3^- peaks, demonstrating that $Cu_{(m)}$ will reduce I_3^-. As a result, $Cu_{(m)}$ must be completely removed from samples derived from lithium-ion battery cells prior to performing the proposed redox titration method.

e. Redox Titration Method for Reduction of Triiodide via Lithium Metal

The feasibility of the proposed redox titration method for the reduction of I_3^- by unpassivated $Li_{(m)}$ remaining in a used, lithium-ion cell was explored. A control test was

performed using a ~5 x 5 x 0.45 mm sample of $Li_{(m)}$ ribbon. The $Li_{(m)}$ sample was added in excess to a $9.75 \cdot 10^{-5}$ M I_3^- in anhydrous PC solution in an Ar purged glovebox, to minimize potential contaminants to the redox reaction between I_3^- and $Li_{(m)}$. UV/vis spectrometry was used to track the reduction of I_3^-.

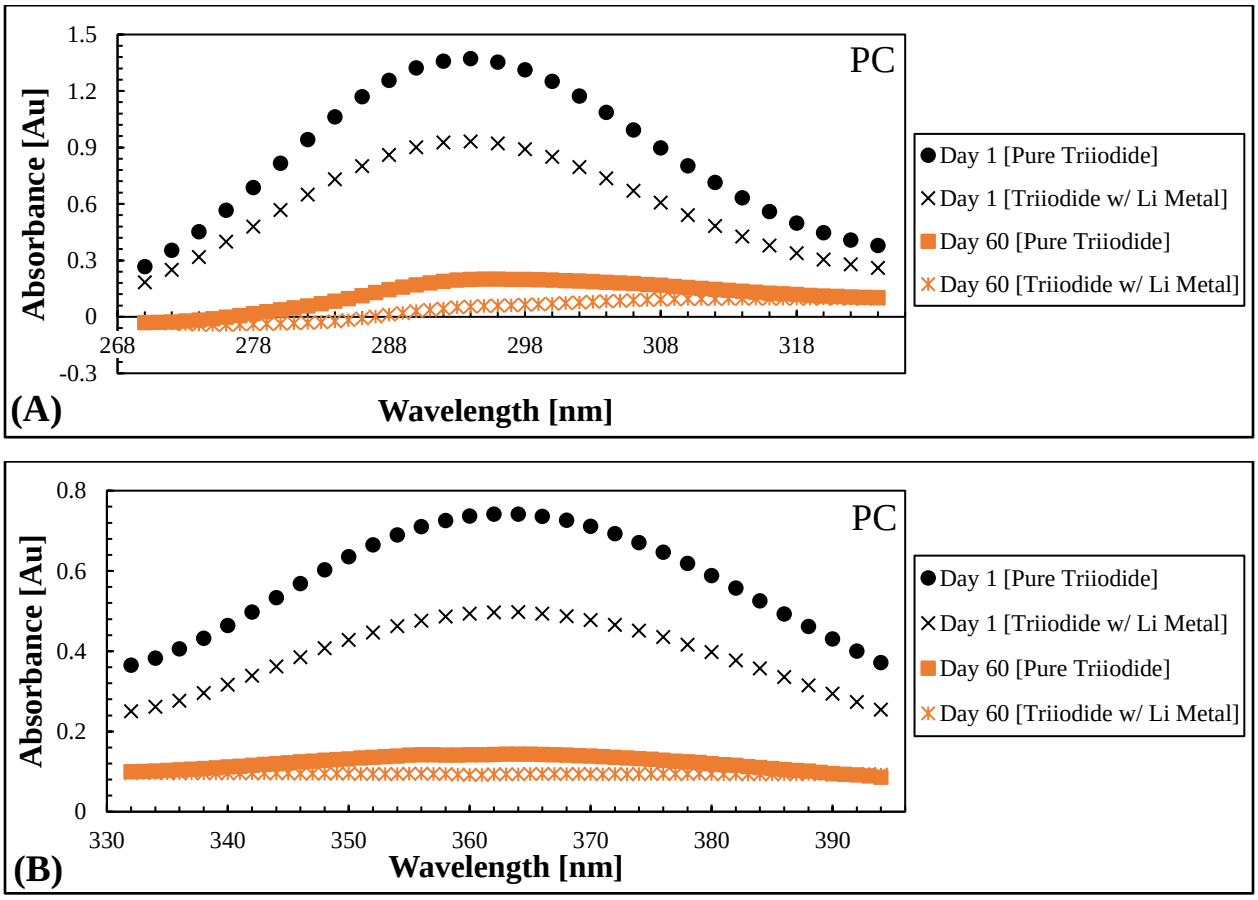

Figure 9. UV/vis spectroscopy results of the first **(A)** and second **(B)** characteristic I_3^- peaks for pure I_3^- samples one day after synthesis (black '○') and 60 days after synthesis (black 'x') as well as I_3^- samples containing $Li_{(m)}$ one day after synthesis (orange '□') and 60 days after synthesis (orange '*'). The I_3^- solution consisted of $9.75 \cdot 10^{-5}$ M I_3^- in PC, stored in an Ar purged glovebox in between sample testing.

The results from the control experiment, as shown above in **Figure 9**, are consistent with the expected reduction reaction. However, the redox reaction kinetics between $Li_{(m)}$ and I_3^- are slow, with significant peak intensities for I_3^- still remaining after one day. At that time, the maximum intensity for the I_3^- containing the $Li_{(m)}$ was determined to be 0.245 au less than the pure I_3^- control sample. The characteristic I_3^- peaks persisted for 60 days, which was expected considering that excess $Li_{(m)}$ was added to I_3^-. The above experiment should be repeated, taking multiple UV/vis measurements each day on the I_3^- samples until the characteristic I_3^- peaks are no longer observed, to fully characterize the kinetics of the redox reaction.

The proposed redox reaction was no longer pursued at this point due to its infeasibility for industry use. An attempt was made to combine a I_3^- in PC solution, within the operable concentration range for UV/vis, with a stoichiometric amount, or less, of $Li_{(m)}$. To achieve this,

an impractical amount of I_3^- in PC solution would be required for a minute amount of $Li_{(m)}$. This is due to the extremely large difference in the molar masses of I_3^- and $Li_{(m)}$, with a molar mass ratio of ~55:1. This means that a 100.0 mL I_3^- sample at the highest suggested concentration for UV/vis, being $1.000 \cdot 10^{-4}$ M I_3^-, would result in a $6.941 \cdot 10^{-5}$ g stoichiometric amount of $Li_{(m)}$. Complications also arose during the long-term stability tests, where $Cu_{(m)}$, a common material used for anode current collectors in lithium-ion batteries, was found to also serve as a reductant for I_3^-. This creates the need for vigorous and potentially hazardous pre-treatment, requiring the removal of any $Cu_{(m)}$ that may be present within the investigated lithium-ion cell, prior to performing the proposed redox titration method. Thus, for the purpose of analyzing the amount of active $Li_{(m)}$ that remains in a used lithium-ion battery, we can conclude that the proposed redox titration method is not practical.

2. pH Titration of Lithium with a Strong Acid

a. pH Titration Method Development

For the pH titration method, candidate solvents DI H_2O and MeOH are reacted with any remaining active $Li_{(m)}$:

$$2Li_{(m)} + 2H_2O_{(l)} \rightarrow 2LiOH_{(aq)} + H_{2(g)} \quad \textbf{(3)}$$

$$2Li_{(m)} + 2CH_3OH_{(l)} \rightarrow 2CH_3OLi_{(l)} + H_{2(g)} \quad \textbf{(5)}$$

in a used lithium-ion cell. The resulting reactions generate a stoichiometric amount of a strong base, either hydroxide (OH^-) or methoxide (CH_3O^-) ions, to the amount of $Li_{(m)}$ added to DI H_2O and MeOH, respectively. Thus, the resulting basic solution can be titrated using a strong acid, such as H_2SO_4:

$$2LiOH_{(aq)} + H_2SO_{4(aq)} \rightarrow Li_2SO_{4(aq)} + 2H_2O_{(l)} \quad \textbf{(4)}$$

$$2CH_3OLi_{(l)} + H_2SO_{4(aq)} \rightarrow Li_2SO_{4(aq)} + 2CH_3OH_{(l)} \quad \textbf{(6)}$$

correlating the amount of titrant required to bring the solution to a neutral pH to the amount of $Li_{(m)}$ added. DI H_2O and MeOH were selected as the best candidate solvents due to their high reactivity with $Li_{(m)}$, as shown in **Table 3**, and their associated conjugate pair being a strong base. A control test was initially performed, using solid LiOH in place of $Li_{(m)}$ to allow for the experiment to take place under ambient conditions. A range of dilutions of LiOH in both DI H_2O and MeOH were titrated in parallel with aqueous H_2SO_4, using a phenolphthalein (phph) indicator to track the pH of the LiOH analyte solutions.

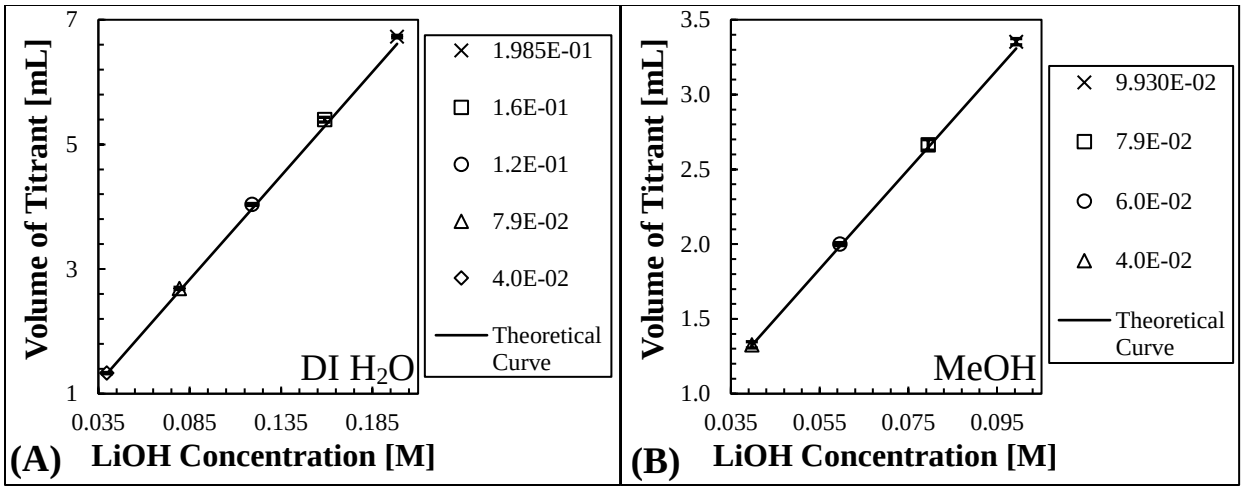

Figure 10. Averaged standard curve results from the control experiment, titrating a range of LiOH dilutions with a $7.50 \cdot 10^{-2}$ M H_2SO_4 in DI H_2O titrant in triplicate. The experimental results are plotted against the theoretical values, using a 2:1 stoichiometric ratio of LiOH to H_2SO_4. (A) The LiOH analyte solutions were diluted in DI H_2O at $1.985 \cdot 10^{-1}$ M (black 'x'), $1.6 \cdot 10^{-1}$ M (black '□'), $1.2 \cdot 10^{-1}$ M (black '○'), $7.9 \cdot 10^{-2}$ M (black 'Δ'), and $4.0 \cdot 10^{-2}$ M (black '◊') concentrations. (B) The LiOH analyte solutions were diluted in MeOH at $9.930 \cdot 10^{-2}$ M (black 'x'), $7.9 \cdot 10^{-2}$ M (black '□'), $6.0 \cdot 10^{-2}$ M (black '○'), and $4.0 \cdot 10^{-2}$ M (black 'Δ') concentrations.

The experimental values from the control experiment followed closely with the theoretical 2:1 stoichiometric ratio for LiOH analyte to H_2SO_4 titrant for both the DI H_2O and MeOH solvent systems, as shown above in **Figure 10**. The average error associated with the DI H_2O solvent system, shown in **Figure 10A**, was determined to be 0.07 ± 0.04 mL of required H_2SO_4 titrant, which results in an average percent error of 2%. At the maximum observed error, determined to be $9 \cdot 10^{-6}$ mol of H_2SO_4, the proposed pH titration method would differ by just $1 \cdot 10^{-4}$ g from the actual mass of $Li_{(m)}$ originally in solution. The MeOH solvent system, shown in **Figure 10B**, proved even more accurate, with an average error of 0.02 ± 0.02 mL or average percent error of just 1%. The experimental values were also determined to be within experimental error of the target value, having a maximum standard deviation of just 0.04 mL between replicate runs for both solvent systems. Thus, the results from the control experiment indicate that the proposed pH titration between aqueous H_2SO_4 and LiOH in both DI H_2O and MeOH offer accurate results with high replicability.

Unfortunately, due to the COVID-19 pandemic, the investigation of the pH titration method was cut short, with the necessary laboratory facilities shutdown to mitigate the spread of the virus. The following discussion, however, serves as a guide for the intended experiments designed to evaluate the feasibility of the pH titration method for determination of active lithium remaining in used lithium-ion batteries. One of the major concerns with the proposed pH titration method is the potential for liberating lithium from compounds associated with passivation within a used cell. This would result in an over-estimation of the remaining active $Li_{(m)}$ within the cell and would be counter-productive to the overall purpose for the quantification method. Characterization of the passivation layer formed on anodes within used lithium-ion batteries have been of significant interest and can vary from cell to cell, depending on the chemical makeup of the electrodes and electrolyte solution.[19, 20] However, it has been determined that the passivation

layer associated with most lithium-ion anodes primarily consist of lithium carbonate (Li_2CO_3) and lithium alkylcarbonates ($ROCO_2Li$).[19, 20] Thus, control experiments should be run, comparing the results between titrated samples of LiOH, LiOH combined with Li_2CO_3, and LiOH combined with $ROCO_2Li$ in both candidate solvent systems. The electrolyte solution may also serve as a potential source for undesired lithium contributions, with common lithium-ion electrolytes consisting of lithium perchlorate ($LiClO_4$), lithium hexafluophosphate ($LiPF_6$), or bis(trifluoromethane)sulfonimide lithium salt ($LiN(SO_2CF_3)_2$).[19] Thus, control experiments should also be conducted, combining common lithium-ion electrolyte compounds with LiOH, to deny their interference with the $Li_{(m)}$ quantification. As previously discussed in the redox titration method development, $Cu_{(m)}$ may serve as competing reductant to $Li_{(m)}$. $Cu_{(m)}$ has not been observed to spontaneously react in weak acids, such as DI H_2O and MeOH, nor are the oxidation kinetics of $Cu_{(m)}$ in DI H_2O and MeOH competitive compared to their reaction with $Li_{(m)}$.[30, 31] While its formation is unlikely, Cu^{2+} has been cited to react with OH^- in aqueous solutions:

$$[Cu(H_2O)_6]^{2+}_{(aq)} + 2OH^-_{(aq)} \rightarrow [Cu(H_2O)_4(OH)_2]_{(s)} + 2H_2O_{(l)} \quad \textbf{(7)}$$

which would affect the stoichiometric ratio of the pH titration method, resulting in an underestimation of $Li_{(m)}$.[32] Thus, control experiments should be conducted, similar to the experiments performed for the redox titration development, comparing titration results from samples containing LiOH to LiOH combined with $Cu_{(m)}$ foil to observe possible interferences with $Cu_{(m)}$ in both solvent systems. A final control experiment should be performed with $Li_{(m)}$ to confirm the stoichiometric formation of OH^- and CH_3O^- when combined with DI H_2O and MeOH, respectively. Once the chemical reactions, described in **Equations (3) and (5)**, are confirmed by the titration with H_2SO_4, the pH titration method can be applied to a new and used lithium-ion cell to confirm its feasibility and effectiveness.

Conclusion.

Recycling of lithium-based battery technologies are crucial for meeting the future surge in demand from the small electronics, automotive, and renewable energy industries. Novel passivation techniques seek to decrease the economic hardships and safety measures required for the handling and transportation of used lithium batteries by decreasing the reactivity of remaining active lithium compounds. The development of a cost-effective and robust quantification method for measuring the amount of active lithium, separate from compounds associated with passivation, aims to verify the success of these techniques, and subsequently lower the hazard classifications for these materials. A redox titration was explored, involving the reduction of triiodide by active lithium in a propylene carbonate or acetonitrile solvent system. While the desired mechanism was observed through ultraviolet-visible spectroscopy, significant downsides stemming from the large difference in molar masses between lithium and triiodide and the competing reductant properties of copper, a common material used for anode current collectors, deemed the method impractical for industry applications. A second, pH titration

technique, which relies on the reaction between lithium and either water or methanol, involved the use of a strong acid to titrate the resulting basic solution. Preliminary experiments for the pH titration method indicated optimistic results for the ability of aqueous sulfuric acid titrant in measuring the amount of lithium hydroxide and lithium methoxide present in solution with high replicability. However, due to the ensuing COVID-19 pandemic, further investigation of the pH titration method was ceased. Additional studies for analyzing potential contaminants to the titration method, such as copper metal, common electrolyte materials, and passivated lithium compounds, should be conducted to determine the feasibility of the technique.

Supplemental Information.

1. Supplemental Tables.

Compound [CAS #]	Manufacturer	Grade/Description	Purity
Methanol [67-56-1]	Sigma Aldrich	ACS	99.8%
n-Butanol [71-36-3]	Sigma Aldrich	ACS	≥99.4%
Acetone [67-64-1]	Sigma Aldrich	Technical	≥99.5%
Acetonitrile [75-05-8]	Fischer Scientific	HPLC	≥99.9%
Propylene Carbonate [108-32-7]	Sigma Aldrich	Reagent	99%
	Sigma Aldrich	Anhydrous	99.8%
Lithium Metal [7439-93-2]	Sigma Aldrich	Ribbon	99.9%
Sodium Thiosulfate [7772-98-7]	Sigma Aldrich	Anhydrous	≥98.0%
Iodine [7553-56-2]	Sigma Aldrich	ACS	99.8%
Potassium Iodide [7681-11-0]	Fischer Scientific	ACS	≥99.0%
Lithium Iodide [10377-51-2]	Sigma Aldrich	Anhydrous	99.9%
Sodium Iodide [7681-82-5]	Sigma Aldrich	Reagent	≥99.5%
Copper Foil [7440-50-8]	-	Foil	-

Table 5. List of referenced reagents used during the redox titration with I_3^- experimentation. Included is the Chemical Abstract Service (CAS) number, manufacturer, grade or description, and purity.

Compound [CAS #]	Manufacturer	Grade/Description	Purity
Methanol [67-56-1]	Sigma Aldrich	ACS	99.8%
Sulfuric Acid [7664-93-9]	Fischer Scientific	ACS	≥95.0%
Lithium Hydroxide [310-65-2]	Fischer Scientific	Anhydrous	98%
Phenolphthalein [77-09-8]	Fischer Scientific	Indicator	1%

Table 6. List of referenced reagents used during the pH titration with LiOH and H_2SO_4 experimentation. Included is the Chemical Abstract Service (CAS) number, manufacturer, grade or description, and purity.

References.

1. Goonan, T. G., Lithium Use in Batteries. Survey, U. S. G., Ed. Circular, 2012; Vol. 1371, p 14.

2. Meesala, Y.; Jena, A.; Chang, H.; Liu, R.-S., Recent Advancements in Li-Ion Conductors for All-Solid-State Li-Ion Batteries. *ACS Energy Letters* **2017,** *2* (12), 2734-2751.

3. Bradley, D. C.; Stillings, L. L.; Jaskula, B. W.; Munk, L.; McCauley, A. D. *Lithium*; 1802K; Reston, VA, 2017; p 34.

4. Dessemond, C.; Lajoie-Leroux, F.; Soucy, G.; Laroche, N.; Magnan, J.-F., Spodumene: The Lithium Market, Resources and Processes. *Minerals* **2019,** *9* (6), 334.

5. Jaskula, B. W., Lithium. Survey, U. S. G., Ed. 2020 Mineral Commodity Summaries, 2020; pp 98-99.

6. Jacoby, M., It's Time to get Serious about Recycling Lithium-Ion Batteries. *Chemical & Engineering News* **2019,** *97* (28).

7. Lithium-Ion Battery Market Analysis by Product, by Application, and Segment Forecasts. Research, G. V., Ed. 2017.

8. Yoshino, A., Development of the Lithium-Ion Battery and Recent Technological Trends. In *Lithium-Ion Batteries*, Pistoia, G., Ed. Elsevier: Amsterdam, 2014; pp 1-20.

9. Shedd, K. B., Cobalt. Survey, U. S. G., Ed. Mineral Commodity Summaries, 2020; pp 50-51.

10. Shedd, K. B., Cobalt. Survey, U. S. G., Ed. 2016 Minerals Yearbook, 2019; Vol. 19.

11. Democratic Republic of Congo Events of 2018. *Human Rights Watch* **2018**.

12. The Hazards of Lithium Batteries. *Tufts EHS Newsletter* **2016,** *8* (1), 3-4.

13. Lithium Hexafluorophosphate. Database, P., Ed. National Center for Biotechnology Information.

14. Lamb, J.; Orendorff, C.; Roth, E.; Langendorf, J., Studies on the Thermal Breakdown of Common Li-Ion Battery Electrolyte Components. *Journal of The Electrochemical Society* **2015,** *162*, A2131-A2135.

15. Hydrofluoric Acid. Database, P., Ed. National Center for Biotechnology Information.

16. Lithium. Database, P., Ed. National Center for Biotechnology Information.

17. Events with Smoke, Fire, Extreme Heat, or Explosion Involving Lithium Batteries. Administration, F. A., Ed. FAA Office of Security and Hazardous Materials Safety: 2020.

18. Gaines, L., Lithium-Ion Battery Recycling Processes: Research Towards a Sustainable Course. *Sustainable Materials and Technologies* **2018,** *17*, e00068.

19. Mori, S.; Asahina, H.; Suzuki, H.; Yonei, A.; Yokoto, K., Chemical Properties of Various Organic Electrolytes for Lithium Rechargeable Batteries: 1. Characterization of Passivating Layer Formed on Graphite in Alkyl Carbonate Solutions. *Journal of Power Sources* **1997,** *68* (1), 59-64.

20. Naji, A.; Ghanbaja, J.; Willmann, P.; Billaud, D., TEM Characterization of the Passivating Layer Formed during the Reduction of Graphite Electrodes in Selected Electrolytes. *Journal of Power Sources* **1999,** *81-82*, 207-211.

21. Sloop, S.; Crandon, L.; Allen, M.; Koetje, K.; Reed, L.; Gaines, L.; Sirisaksoontorn, W.; Lerner, M., A Direct Recycling Case Study from a Lithium-Ion Battery Recall. *Sustainable Materials and Technologies* **2020,** *25*, e00152.

22. Kim, H., The Insertion Mechanism of Lithium into Mg_2Si Anode Material for Li-Ion Batteries. *Journal of The Electrochemical Society* **1999,** *146* (12), 4401.

23. Zhao, Q.; Lu, Y.; Zhu, Z.; Tao, Z.; Chen, J., Rechargeable Lithium-Iodine Batteries with Iodine/Nanoporous Carbon Cathode. *Nano Lett* **2015,** *15* (9), 5982-7.

24. Wei, Y. J.; Liu, C. G.; Mo, L. P., Ultraviolet Absorption Spectra of Iodine, Iodide Ion and Triiodide Ion. *Guang Pu Xue Yu Guang Pu Fen Xi* **2005,** *25* (1), 86-8.

25. Sigma, M., Solvent Miscibility Table. Merck KGaA: 2020.

26. Riddick, J. A.; Bunger, W. B.; Sakano, T. K., *Organic Solvents: Physical Properties and Methods of Purification*. 4 ed.; John Wiley and Sons,New York, NY: United States, 1986.

27. Asakai, T.; Hioki, A., Investigation of Iodine Liberation Process in Redox Titration of Potassium Iodate with Sodium Thiosulfate. *Anal Chim Acta* **2011,** *689* (1), 34-8.

28. Clayton, G. D.; Clayton, F. E., *Patty's Industrial Hygiene and Toxicology*. 4 ed.; John Wiley & Sons: 1995; Vol. 15, p 421-421.

29. Ramette, R. W.; Sandford, R. W., Thermodynamics of Iodine Solubility and Triiodide Ion Formation in Water and in Deuterium Oxide. *Journal of the American Chemical Society* **1965,** *87* (22), 5001-5005.

30. Yang, J. C.; Bharadwaj, M. D.; Zhou, G.; Tropia, L., Surface Kinetics of Copper Oxidation Investigated by In Situ Ultra-high Vacuum Transmission Electron Microscopy. *Microsc Microanal* **2001,** *7* (6), 486-493.

31. Bluhm, H.; Hävecker, M.; Knop-Gericke, A.; Kleimenov, E.; Schlögl, R.; Teschner, D.; Bukhtiyarov, V. I.; Ogletree, D. F.; Salmeron, M., Methanol Oxidation on a Copper Catalyst Investigated Using in Situ X-ray Photoelectron Spectroscopy. *The Journal of Physical Chemistry B* **2004,** *108* (38), 14340-14347.

32. Clark, J.; Shrestha, B., *Chemistry of Copper*. 2019.